ACS APPLIED MATERIALS & INTERFACES

Research Article

www.acsami.org

Voltage-Gated Transport of Nanoparticles across Free-Standing All-Carbon-Nanotube-Based Hollow-Fiber Membranes

Gaoliang Wei, Xie Quan,* Shuo Chen, Xinfei Fan, Hongtao Yu, and Huimin Zhao

Key Laboratory of Industrial Ecology and Environmental Engineering (Ministry of Education, China), School of Environmental Science and Technology, Dalian University of Technology, Dalian 116024, China

Supporting Information

ABSTRACT: Understanding the mechanism underlying controllable transmembrane transport observed in biological membranes benefits the development of next-generation separation membranes for a variety of important applications. In this work, on the basis of common structural features of cell membranes, a very simple biomimetic membrane system exhibiting gated transmembrane performance has been constructed using all-carbon-nanotube (CNT)-based hollow-fiber membranes. The conductive CNT membranes with hydrophobic pore channels can be positively or negatively charged and are consequently capable of regulating the transport of nanoparticles across their pore channels by their "opening" or "closing". The switch between penetration and rejection of nanoparticles through/by CNT membranes is of high efficiency and especially allows dynamic control. The underlying mechanism is that CNT pore channels with different polarities can prompt or prevent the formation of their noncovalent interactions with charged nanoparticles, resulting in their rejection or penetration by/through the CNT membranes. The theory about noncovalent interactions and charged pore channels may provide new insight into understanding the complicated ionically and bimolecularly gated transport across cell membranes and can contribute to many other important applications beyond the water purification and resource recovery demonstrated in this study.

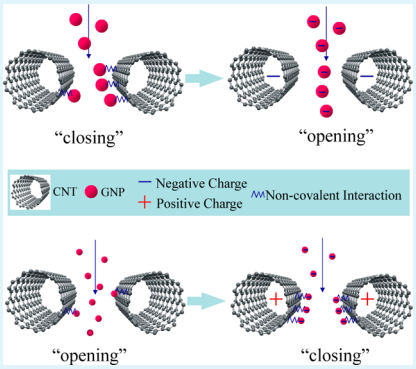

KEYWORDS: *carbon nanotubes, gated transport, membranes, voltage, noncovalent interaction*

INTRODUCTION

Biological membranes regulate cellular traffic connecting the internal environment with the outside, often with high selectivity and high efficiency. These ultraprecision biological machines achieve rapid, selective transmembrane mass transport and gated processes by employing a large variety of specialized protein channels.[1] These channels of nanometer or subnanometer size share several common structural features including a hydrophobic inner surface[2−4] and charged functional groups in the selectivity filter regions.[1] Many studies, on the basis of this information, have been devoted to mimicking these ultraefficient biological systems with artificial nanophase materials, aiming at understanding the underlying mechanisms responsible for the fast mass transport, selectivity, and gating as well as creating next-generation membranes supporting efficient water permeability and high mass selectivity.[5−16]

Molecular dynamics simulations have proposed carbon nanotubes (CNTs) as ideal candidates for such simplified models of biological channels and have demonstrated the single-file transport of water molecules along the CNTs axis[5−8] that is designed as protein channels. Theoretically predicted and experimentally measured water transport rates through CNTs are extremely large and comparable to the measured values for aquaporins.[8−10] Introducing oxygen-containing functional groups to the CNT nanotube entrance can create an artificial selectivity region that can govern ion or molecular rejection when aqueous solutions pass through the pores.[1,11−13] Carboxylic-group-containing open tips of CNTs can be further easily derivatized with a ligand molecule (for example, desthiobiotin derivatives[14] and phosphorylated serine[15]) that binds to a bulky receptor, thereby enabling a reversible "closing"/"opening" of the core entrance. The membranes, composed of an array of aligned CNTs and functionalized with charged molecular tethers, can also exhibit gated transport under assistance of voltage, which is achieved by controlling the tethered charge molecules to close or open the CNT cores.[16] Despite the enormous efforts made in recent decades, the detailed processes of gated transport have not been fully understood because of the complex physicochemical nature of these biological channels. Additionally, the biomimetic systems constructed with these microfabricated membranes are still complicated, and the switch between closing and opening of pores in these membranes is of low efficiency. Thus, it is important to create more simplified and robust biomimetic channels that help to clarify the interactions of targets with them as well as create the next-generation advanced membranes for practical applications.

Received: February 6, 2015
Accepted: June 24, 2015
Published: June 24, 2015

DOI: 10.1021/acsami.5b01183
ACS Appl. Mater. Interfaces 2015, 7, 14620−14627

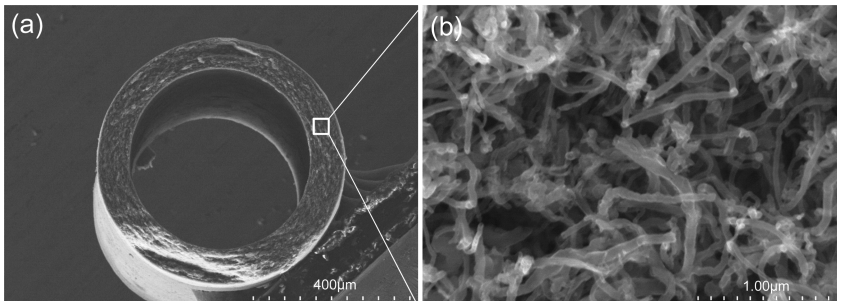

Figure 1. SEM images of (a) cross section and (b) pore channels of a CNT hollow-fiber membrane.

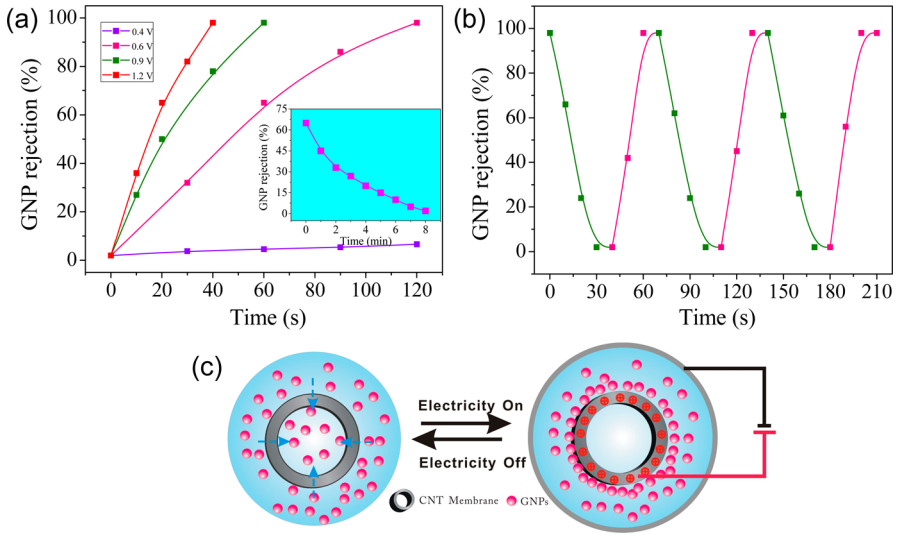

Figure 2. (a) GNP rejection as a function of duration at different voltages. Inset: GNP rejection as a function of duration in absence of voltage. (b) Continuous dynamic switches between permeation and rejection of GNPs through/by CNT membranes (red curve: electricity on; green curve: electricity off). Operational conditions in a and b: flow rate = 10 mL cm^{-2} h^{-1}, transmembrane pressure = 0.002 MPa. (c) Schematic illustration for the switch between opening and closing of membrane pores for 10 nm GNPs.

Herein, we demonstrate that all-CNT-based membranes with well-defined hollow-fiber configuration and hydrophobic pore channels can be employed to construct a very simple biomimetic membrane system showing voltage-gated transport of nanoparticles across their pore channels. In this system, positively or negatively charged pore channels are obtained by application of polarity-difference external bias to the CNT membranes. We also investigate the fundamental mechanisms governing the gated transport of nanoparticles. Although it is generally recognized that endocytosis and exocytosis are the transmembrane approach and that nanoparticles may not penetrate the membrane of a cell through protein channels, this system may provide new insight into understanding how biological pore channels interact with targets and how the charges effect the interactions. In addition, the unique function of CNT hollow-fiber membranes demonstrated in this work will open immense potentials for broad and practical applications.

EXPERIMENTAL SECTION

Surface Functionalization of CNTs. Briefly, 4 g of multiwalled CNTs (60−100 nm in outer diameter, obtained from Shenzhen Nanotech Port Co., Ltd., China) were added to 160 mL of HNO_3/H_2SO_4 (1:3, v/v) concentrated solution that was subsequently heated to 60 °C for 30 min under stirring. After the mixture was diluted with about 2000 mL of water, the CNTs were recovered by filtration with polyvinylidene fluoride microfiltration membrane discs (average pore size = 0.45 μm), followed by being washed with *N*,*N*-dimethylformamide and water in sequence until the pH of the CNT dispersion was nearly neutral. Then, the CNTs were recovered again and dried at 60 °C for 12 h.

Preparation of CNT Hollow-Fiber Membranes. The CNT hollow-fiber membranes were prepared by a technique based on an electrophoretic deposition process reported in our previous work.[17] The obtained membranes were subsequently calcined in a flow of Ar (40 sccm) and H_2 (10 sccm) at 1000 °C for 2 h to remove oxygen-containing functional groups.

Synthesis of 10 nm GNPs. GNPs with a average diameter of about 10 nm were synthesized with the method described by Bastús.[18] In a typical procedure, a solution of 2.2 mM sodium citrate in 150 mL of ultrapure water was heated to boiling for 10 min in a 250 mL three-necked round-bottomed flask equipped with a condenser under vigorous stirring. Then, 1 mL of 25 mM $HAuCl_4$ was injected, and the solution was kept at boiling for another 10 min. The transmission electron microscopy (TEM) image of prepared GNPs is shown in Figure S1.

Synthesis of 40 nm GNPs. Briefly, 1 mL of 25 mM $HAuCl_4$ was diluted into 100 mL of solution with ultrapure water, and the solution was heated to boiling for 10 min in a 250 mL three-necked round-bottomed flask. Then, 1.5 mL of 1 wt % sodium citrate solution was injected, and the solution was kept at boiling for another 10 min. The SEM image of prepared GNPs is shown in Figure S2.

RESULTS AND DISCUSSION

Design for the Biomimetic Membrane System. CNT-based membranes are chosen to construct the biomimetic

DOI: 10.1021/acsami.5b01183
ACS Appl. Mater. Interfaces 2015, 7, 14620−14627

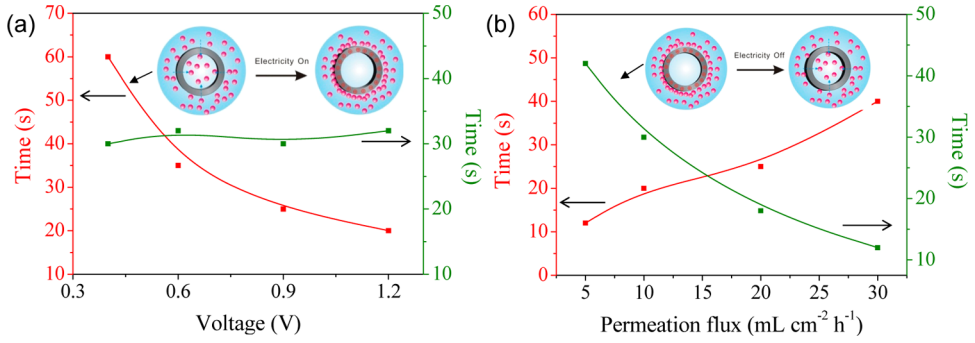

Figure 3. Effects of (a) voltage and (b) permeation flow rate on the rates of switch between permeation and rejection. Red curve represents the switch from permeation to rejection in the presence of electricity; green curve represents the switch from rejection to permeation in absence of electricity. Permeation flow rate in a is 10 mL cm^{-2} h^{-1}; voltage in b is 1.2 V.

membrane system in view of their sharing common structural features with a cell membrane. These CNT membranes typically feature a well-defined hollow-fiber configuration (Figure 1a) and random pore channels (Figure 1b). They also demonstrate good electric conductivity (~1.4 S m^{-1}), considerable tensile strength (8.5 MPa, Figure S3), and bearable maximum transmembrane pressure of >0.5 MPa (Figure S4). To eliminate any potential influence of charged groups, the prepared CNT hollow-fiber membranes are subsequently subjected to calcination in a flow of Ar (40 sccm) and H_2 (10 sccm) at 1000 °C for 2 h to remove oxygen-containing groups that are introduced during their preparation process. X-ray photoelectron spectroscopy (XPS) analysis (Figure S5) indicates an oxygen content of as low as 2.18% of these CNT membranes after thermal treatment, ensuring negligibly intrinsically charged surfaces in water.

Subsequently, a two-electrode system with CNT hollow-fiber membranes as work electrode and a stainless-steel network as counter electrode is constructed to impart reversibly negatively or positively charged CNT pore channels. In this system, the network is bent into a cylinder with CNT hollow-fiber membranes positioned in its axis and at a distance from them of 0.5 cm (Figure S6a). The space charge at the membrane interface is manipulated by the application of a voltage. To eliminate any potential influence of change in transmembrane flow rate, the system is performed at dead-end filtration mode with constant flow rates (milliliter per square centimeter of membrane area per hour) provided by a high-pressure constant-flow pump (Figure S6b). Gold nanoparticles (GNPs) with well-defined diameters are chosen as a model nanoparticle because of their easily regulated sizes and charged surface.

Opening–Closing Switch of Membrane Pores for 10 nm Nanoprticles. The diameters of nanoparticles relative to pore size, which usually determines their interactions with pore channels, will greatly influence their transport dynamics across a membrane. Consequently, transport selectivity for 10 nm GNPs (zeta potential = −28 mV, pH 6.2), which are much smaller than membrane pore size (average 120 nm, Figure S7), is first investigated. To quantify the selectivity, concentrations of GNPs in feed and filtrate are determined by UV–vis spectroscopy. As shown in the inset of Figure 2a, in absence of voltage, CNT hollow-fiber membranes achieve an initial GNP rejection of 65% at a permeation flow rate of 10 mL cm^{-2} h^{-1}, and it decreases to <5% after an operation of 8 min. Then, a voltage of 0.6 V is applied on the biomimic membrane system (CNT membranes as anode). Interestingly, the GNP rejection rapidly increases to >98% from an initial measurement of <5% in 120 s (Figure 2a). If the voltage is decreased to 0.4 V, then GNP rejection only increases to 7% after an operation of same 120 s, and selectivity improvement cannot be observed with further decreasing the voltage, demonstrating a threshold voltage of about 0.4 V inspiring the GNP rejection. In contrast, if the voltages are increased to 0.9 and 1.2 V, then GNP rejection can also improve to >98% but in much shorter durations (60 and 40 s, respectively). These results obviously indicate that higher voltage will bring about more efficient improvement in GNP selectivity. To investigate whether the improved selectivity can be reversed, we continue the operation with shutting off the voltage, using the CNT membranes under previous observation at 1.2 V. As shown in Figure 2b, GNP rejection sharply decreases to <5% in 30 s, and if the electricity is turned on again, then it increases to >98% in an even shorter duration (20 s). The efficient and dynamic switches between permeation and rejection of GNPs through/by CNT membranes can be continuously performed for many times (Figure 2b). Voltage is thus considered to regulate the transport of nanoparticles across the CNT membranes by opening or closing the membrane pores as a gate keeper (schematically shown in Figure 2c): In absence of voltage, the GNPs can freely penetrate the CNT membranes, but in the presence of voltage, the GNPs can be rejected by CNT membranes. We also have investigated the rejection ability of CNT membranes with negative potential. It is found that no obvious improvement in GNP rejection is observed when a voltage of 1.0 V is applied on the biomimic membrane system (CNT membranes as cathode).

Gated transport behavior observed in biomembrane system is believed to correlate with physical or chemical interactions (for example, between ions and pores) influenced by changes in ligand binding, temperature, transmembrane voltage, and mechanical stress.[2,19,20] Similar interactions between targets and CNT pore channels may also exist and could be influenced by operation parameters, for example, applied voltages and permeation flow rates. The changes in these two factors, similar to the biologic stimuli to cell membranes, can influence the efficiency of switches between permeation and rejection of nanoparticles. As shown in Figure 3a, it takes about 20 s for CNT membranes to achieve a GNP rejection of >98% from an initial measurement of <5% at 1.2 V, and the time increases to about 60 s by decreasing the applied voltage to 0.4 V (Figure 3a), suggesting that higher voltage leads to a more rapid switch from permeation to rejection of GNPs through/by CNT membranes. As shown in Figure 3b, the "rejection to

DOI: 10.1021/acsami.5b01183
ACS Appl. Mater. Interfaces 2015, 7, 14620–14627

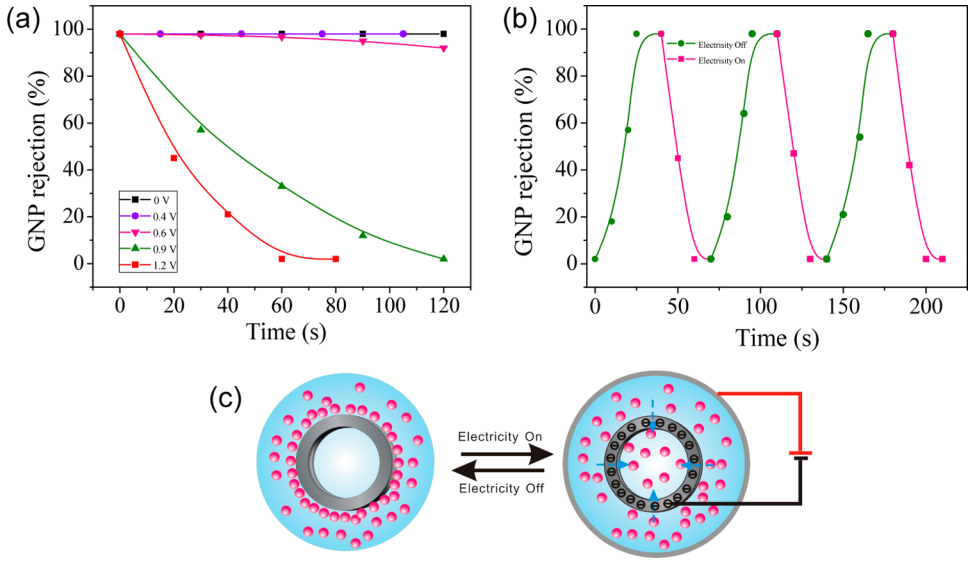

Figure 4. (a) GNP rejection as a function of duration at different voltages. (b) Continuous dynamic switches between rejection and permeation of GNPs by/through CNT membranes (green curve: electricity off; red curve: electricity on). Operational conditions in a and b: flow rate = 10 mL cm^{-2} h^{-1}, transmembrane pressure = 0.002 MPa. (c) Schematic illustration for the switch between closing and opening of membrane pores for 40 nm GNPs.

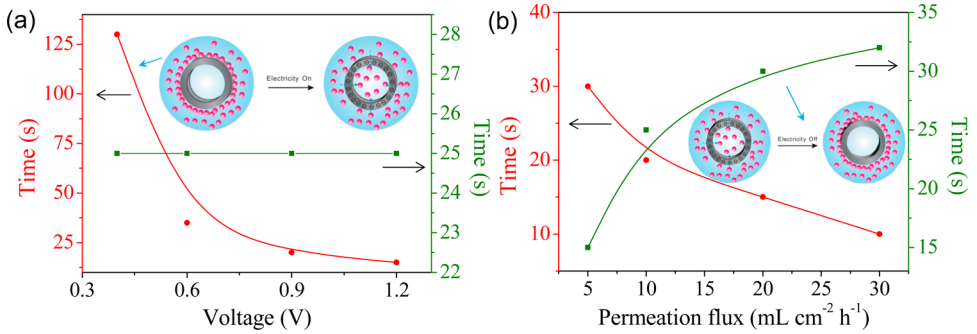

Figure 5. Effects of (a) voltage and (b) permeation flow rate on the rates of switch between permeation and rejection. Red curve represents the switch from rejection to permeation in the presence of electricity; green curve represents the switch from permeation to rejection in absence of electricity. Permeation flow rate in a is 10 mL cm^{-2} h^{-1}; voltage in b is 1.2 V.

permeation" switch is more efficient with the increase of permeation flow rate. Contrarily, the "permeation to rejection" switch is less efficient with increasing the permeation flow rate, which indicates low permeation flow rate is favorable for the rejection of GNPs. Because of its linear relationship with flow rate (Figure S8), transmembrane pressure demonstrates no essential difference in influencing electricity-controlled transport of nanoparticles from flow rate. Therefore, in this work, its influence on gated transport is not additionally investigated.

Closing–Opening Switch of Membrane Pores for 40 nm Nanoprticles. It is generally recognized that transport selectivity, on the basis of chemical or physical property of the nanoparticles, is often observed when they are sufficiently large in size and thereby capable of interacting with pore surface. Thus, GNPs with larger size (average size = 40 nm, zeta potential = −34 mV, pH 5.6) are also employed to further understand the gated transport behavior. As shown in Figure 4a, >98% of 40 nm GNPs can be rejected in the absence of electricity at a permeation flow rate of 10 mL cm^{-2} h^{-1}. If a voltage of 1.0 V is applied on the biomimetic membrane system (CNT membranes as anode), then >98% GNPs can be also rejected. However, with CNT membranes as cathode, the GNP rejection rapidly declines to 8% in 120 s at 0.6 V. It is also obviously exhibited in Figure 4a that higher voltage results in more rapid decline in GNP rejection. Specifically, if the voltage is increased to 1.2 V, then GNP rejection sharply decreases to <5% in 60 s. However, at a voltage below 0.6 V (for example, 0.4 V, Figure 4a), no obvious decrease in GNP rejection is observed, demonstrating a threshold voltage of about 0.6 V inspiring the decline in GNP rejection. Similarly, after shutting off the voltage, we continue the operation using the CNT membranes under previous observation at 1.2 V and find that GNP rejection sharply increases to >98% in 25 s (Figure 4b). If the voltage is turned on again, then it decreases to <5% in an even shorter duration of 20 s. By turning on and off the electricity, the efficient and dynamic switches can be continuously carried out many times (Figure 4b). These results further confirm that the voltage, as a gate keeper, can regulate the transport of nanoparticles across the CNT membranes by opening or closing the membrane pores (schematically shown in Figure 4c): In absence of voltage, the GNPs can be rejected by CNT membrane, and in the presence of voltage, they can freely penetrate the CNT membrane.

The effects of voltage and permeation flow rate on the switch between penetration and rejection are further investigated. It is found that the efficiency of switch from rejection to penetration

DOI: 10.1021/acsami.5b01183
ACS Appl. Mater. Interfaces 2015, 7, 14620−14627

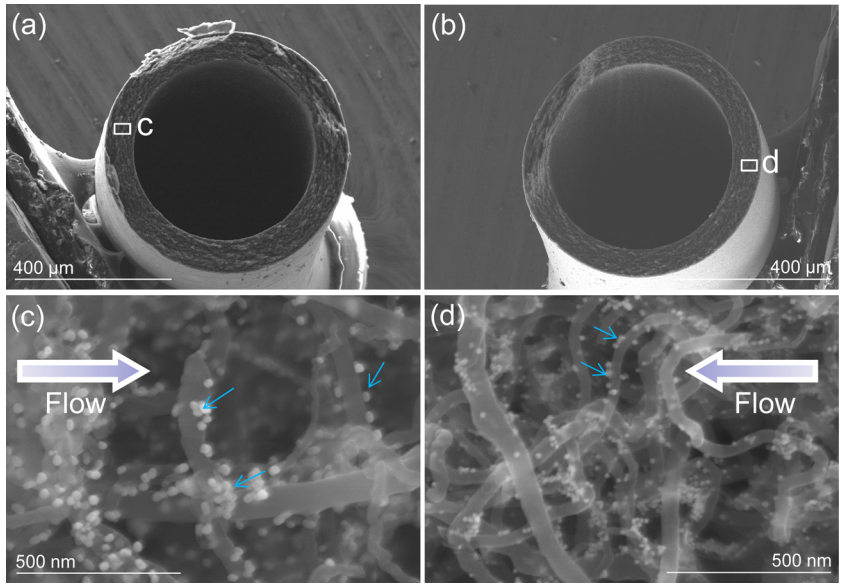

Figure 6. SEM images of CNT hollow-fiber membranes with rejected (a and c) 40 nm GNPs and (b and d) 10 nm GNPs.

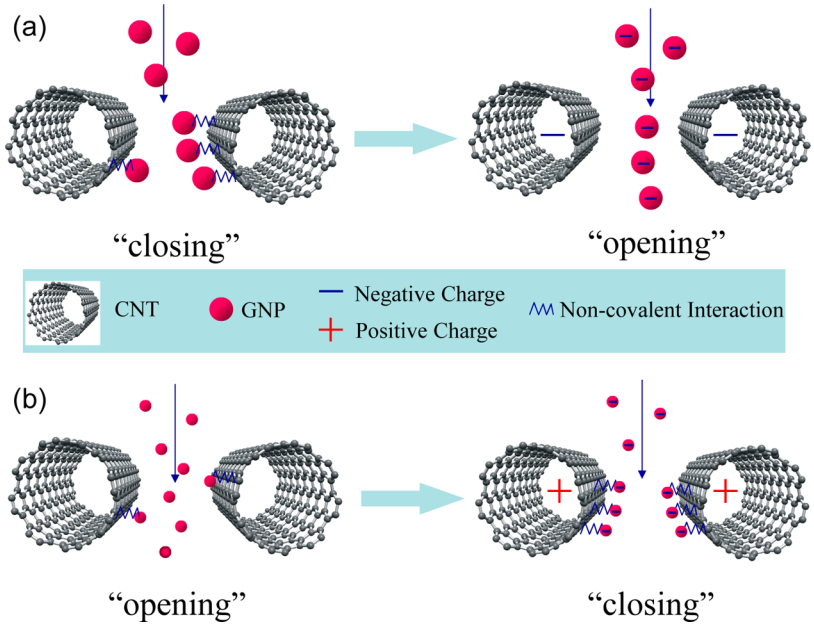

Figure 7. Schematic illustration of mechanism responsible for the voltage-gated transport of nanoparticles across CNT membranes. Electricity-induced switch from (a) closing to opening of membrane pores for 40 nm nanoparticles and (b) opening to closing of membrane pores for 10 nm nanoparticles.

improves with the increase of voltage (Figure 5a), indicating that higher voltage is more favorable for 40 nm GNPs to transport through the membranes. It is also found that permeation flow rate has a great effluence on both the rejection to permeation switch and the permeation to rejection switch. As shown in Figure 5b, it takes 30 s to achieve a rejection to permeation switch at 5 mL cm^{-2} h^{-1}, but the time decreases to about 10 s if the permeation flow rate increases to 30 mL cm^{-2} h^{-1}. In contrast, with the increase of permeation flow rate, the permeation to rejection switch will be less efficient. For instance, at a permeation flow rate of 5 mL cm^{-2} h^{-1}, the permeation to rejection switch can be completed in about 6 s, but the time increases to 34 s at 30 mL cm^{-2} h^{-1}. It is therefore believed that voltage and permeation flow rate influence the switch efficiency by affecting some kinds of interactions between GNPs and pore channels. The detailed mechanism will be discussed in the next section.

Mechanistic Study on Gated Transport of Nanoparticles across CNT-Based Membranes. The transport of specific molecules or ions across the channels embedded in a cell membrane is generally regulated by various stimuli, including membrane potential (voltage-gated channels), chemical ligand (ligand-gated channels), and movement of ligand substructures (mechanically gated channels). SEM characterization indicates that CNT membranes display no obvious structural differences before and after being charged, suggesting the gated transport demonstrated in this work is not attributed to the mechanical opening or closing of CNT channels. The morphology of the CNT membrane with rejected 40 nm GNPs is also characterized by SEM. As

DOI: 10.1021/acsami.5b01183
ACS Appl. Mater. Interfaces 2015, 7, 14620−14627

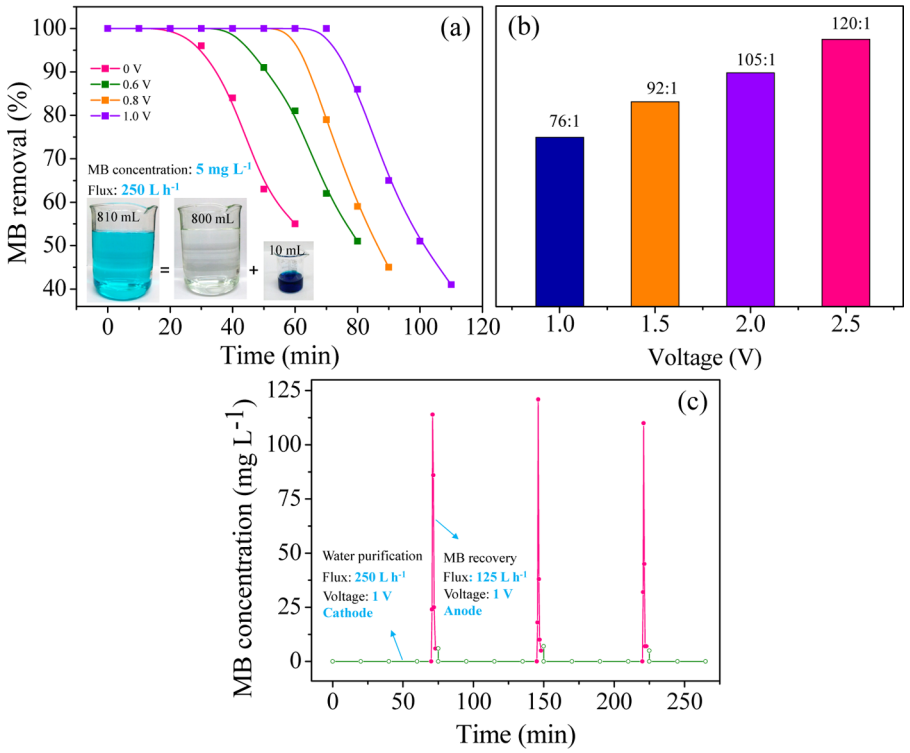

Figure 8. (a) MB removal (%) as a function of time at different voltages. (b) Concentration ratios as a function of voltages. (c) Continuous MB removal and recovery by changing the polarities of CNT membranes. MB concentration in feed, 5 mg L^{-1}; Na_2SO_4 concentration, 0.1 mol L^{-1}; pH 7; total membrane mass, about 500 mg.

shown in Figure 6a,c, in sample area revealing internal pores, many GNPs are decorated around an individual CNT. Obviously, some GNPs attach on the CNT surface following the flow direction, implying that mechanical sieving is not the exclusive or even the main approach for the rejection of GNPs. It is considered that because of the citric acid groups grafted on the GNP surface some noncovalent interactions for example hydrogen bonding and van der Waals forces may form between GNPs and pore channels which are also expected to contribute to their rejection. To further confirm this inference, a new filtration test is performed in the absence of voltage (Figure S9). The result shows that in the first 30 min >98% of 40 nm GNPs can be rejected, but by continuing the operation, some GNPs can successfully penetrate the membranes. The result evidentially supports this inference and can be explained by the fact that they will penetrate the CNT membranes once all the active sites for GNP attachment have been occupied. Similarly, 10 nm GNP can also noncovalently attach on an individual CNT, as shown in Figure 6b,d. All the results suggest that the noncovalent attachment dominates the trap of GNPs by CNT membranes.

After clarifying the reason for the rejection of GNPs, we propose two models accounting for the gated transport on the basis of above results. In the first model (schematically shown in Figure 7a), in absence of electricity, 40 nm GNPs cannot penetrate the CNT membranes because of their interactions with pore channels, implying the pores are closed for these nanoparticles. However, once a negative potential is applied on the CNT membranes, electrostatic repulsion between pore channels and similarly negatively charged GNPs will inhibit the formation of noncovalent interactions between them, and then GNPs can penetrate the open pores. For 10 nm GNPs involved in the other model (Figure 7b), they are sufficiently small in size and beyond the distance of interacting with pore channels in absence of electricity; as a result, they can freely penetrate the open pores of CNT membranes. However, if given a positive potential, then the pore channels can attract negative GNPs, promoting the formation of the noncovalent interactions; thus, GNPs are rejected by closed pores. Hydrophobic pore channels without charged functional groups have eliminated the influence on their interactions with GNPs as much as possible. Voltage controls the polarity of pore channels in CNT membranes and consequently regulates the noncovalent interactions that perform as ligand embedded in protein channels of cell membranes. On the basis of the models, voltage and permeation flow rate will have a great effect on the efficiencies of permeation to rejection and rejection to permeation switches as they influence the formation of the noncovalent interactions. Indeed, the theoretical analysis is consistent with experimental observations shown in Figures 3 and 5. It should be emphasized that apart from the metallic GNPs the transport across the CNT membranes of nonmetallic polystyrene nanoparticles also demonstrates the gated behavior which is also attributed to their noncovalent interactions with pore channels through van der Waals forces or/and $\pi-\pi$ stacking.

Potential Applications for Water Purification and Resource Recovery. The biomimetic membrane system and the gated transport mechanism not only benefit the advancement of membrane science but also are expected to contribute to many other important areas of application, such as microfluidics, controlled drug delivery, and biological science, benefiting from their easy preparation and the versatility of proposed mechanism. Specifically, we will demonstrate in this work the important applications for water purification and resource recovery that have caught global attention. Taking

DOI: 10.1021/acsami.5b01183
ACS Appl. Mater. Interfaces 2015, 7, 14620−14627

methylene blue (MB) molecules as a proof-of-concept, we show that they can be efficiently removed from the water by the CNT membranes, by virtue of the enhanced noncovalent interactions, and recovered by destroying the interactions. To quantify the MB removal and recovery, concentrations of MB in feed and filtrate are determined by UV−vis spectroscopy. As shown in Figure 8a, the CNT membranes can almost completely (>98%) remove MB molecules (initial concentration = 5 mg L^{-1}) before 20 min (defined as penetrating time). If a voltage of 0.6 V is applied on the system (CNT membranes as cathode), then penetrating time increases to about 43 min, which will further increase to 60 and 75 min, respectively, at 0.8 and 1.0 V (Figure 8a), as a result of promotional formation of the interactions. Interestingly, if the CNT membranes are positively charged, then these noncovalent interactions can be easily and rapidly broken, and the MB molecules will be desorbed from CNT channels, achieving the recovery of MB molecules (inset, Figure 8a). It is also observed that the difficulty in fracture of these interactions decreases with increasing the voltage; as a result, the cocentration ratio λ ($\lambda = c_{effluent}/c_{feed}$, where $c_{effluent}$ is the concentration of MB after desorption, and c_{feed} is the concentration of MB in feed (5 mg L^{-1})) increases with the increasing voltage (Figure 8b). Additionlly, the recovery of MB can renew the interfaces in CNT channels at the same time for trapping contaminant molecules again (Figure 8c), thus providing an efficient strategy for water treatment and resource recovery by changing the polarities of CNT membranes.

CONCLUSIONS

As revealed, the all-CNT-based hollow-fiber membranes can perform as biomimic membranes exhibiting voltage-gated transmembrane behavior over nanoparticles by sharing several common structural features with biological membranes in the selectivity filter regions. The efficient, dynamic, and reversible switches between penetration and rejection for nanoparticles are controlled by applied voltages that regulate the transport of nanoparticles across the CNT membranes by opening or closing the pore channels. The noncovalent interactions of nanoparticles with pore channels, of which formation and breakage are determined by the polarity of pore charges, are essentially responsible for the voltage-gated transmembrane phenomenon. Understanding the underlying mechanism will provide the basis for the design of other advanced membranes with ionically and molecularly gated transport channels. Additionally, this work also confirms that these all-CNT hollow-fiber membranes possess distinct advantages over traditional membranes and demonstrates their potential as next-generation advanced membranes for various important areas of application.

ASSOCIATED CONTENT

Supporting Information

TEM image of 10 nm GNPs; SEM image of 40 nm GNPs; XPS analysis, tensile test, pore size analysis, and maximum transmembrane pressure analysis of CNT hollow-fiber membrane; flux as a function of pressure; the experimental setup; GNP (40 nm) rejection as a function of operation time in absence of electricity. The Supporting Information is available free of charge on the ACS Publications website at DOI: 10.1021/acsami.5b01183.

AUTHOR INFORMATION

Corresponding Author

*E-mail: quanxie@dlut.edu.cn. Phone: +86-411-84706140. Fax: +86-411-84706263.

Notes

The authors declare no competing financial interest.

ACKNOWLEDGMENTS

This work was financially supported by National Basic Research Program of China (2011CB936002) and National Natural Science Foundation of China (No.21437001) and PCSIRT_13R05.

REFERENCES

(1) Fornasiero, F.; Park, H. G.; Holt, J. K.; Stadermann, M.; Grigoropoulos, C. P.; Noy, A.; Bakajin, O. Ion Exclusion by Sub-2-nm Carbon Nanotube Pores. *Proc. Natl. Acad. Sci. U. S. A.* **2008**, *105*, 17250−17255.

(2) Bass, R. B.; Strop, P.; Barclay, M.; Rees, D. C. Crystal Structure of *Escherichia coli* MscS, a Voltage-Modulated and Mechanosensitive Channel. *Science* **2002**, *298*, 1582−1587.

(3) Jiang, Y. X.; Lee, A.; Chen, J. Y.; Cadene, M.; Chait, B. T.; MacKinnon, R. Crystal Structure and Mechanism of a Calcium-Gated Potassium Channel. *Nature* **2002**, *417*, 515−522.

(4) Miyazawa, A.; Fujiyoshi, Y.; Unwin, N. Structure and Gating Mechanism of the Acetylcholine Receptor Pore. *Nature* **2003**, *423*, 949−955.

(5) Liu, B.; Li, X. Y.; Li, B. L.; Xu, B. Q.; Zhao, Y. L. Carbon Nanotube Based Artificial Water Channel Protein: Membrane Perturbation and Water Transportation. *Nano Lett.* **2009**, *9*, 1386−1394.

(6) Zuo, G. C.; Shen, R.; Ma, S. J.; Guo, W. L. Transport Properties of Single-File Water Molecules inside a Carbon Nanotube Biomimicking Water Channel. *ACS Nano* **2010**, *4*, 205−210.

(7) Berezhkovskii, A.; Hummer, G. Single-File Transport of Water Molecules through a Carbon Nanotube. *Phys. Rev. Lett.* **2002**, *89*, 064503.

(8) Hummer, G.; Rasaiah, J. C.; Noworyta, J. P. Water Conduction through the Hydrophobic Channel of a Carbon Nanotube. *Nature* **2001**, *414*, 188−190.

(9) Majumder, M.; Chopra, N.; Andrews, R.; Hinds, B. J. Nanoscale Hydrodynamics: Enhanced Flow in Carbon Nanotubes. *Nature* **2005**, *438*, 44.

(10) Holt, J. K.; Park, H. G.; Wang, Y.; Stadermann, M.; Artyukhin, A. B.; Grigoropoulos, C. P.; Noy, A.; Bakajin, O. Fast Mass Transport through Sub−2-Nanometer Carbon Nanotubes. *Science* **2006**, *312*, 1034−1037.

(11) Hinds, B. J.; Chopra, N.; Rantell, T.; Andrews, R.; Gavalas, V.; Bachas, L. G. Aligned Multiwalled Carbon Nanotube Membranes. *Science* **2004**, *303*, 62−65.

(12) Majumder, M.; Chopra, N.; Hinds, B. J. Effect of Tip Functionalization on Transport through Vertically Oriented Carbon Nanotube Membranes. *J. Am. Chem. Soc.* **2005**, *127*, 9062−9070.

(13) Corry, B. Water and Ion Transport through Functionalised Carbon Nanotubes: Implications for Desalination Technology. *Energy Environ. Sci.* **2011**, *4*, 751−759.

(14) Nednoor, P.; Chopra, N.; Gavalas, V.; Bachas, L. G.; Hinds, B. J. Reversible Biochemical Switching of Ionic Transport through Aligned Carbon Nanotube Membranes. *Chem. Mater.* **2005**, *17*, 3595−3599.

(15) Nednoor, P.; Gavalas, V. G.; Chopra, N.; Hinds, B. J.; Bachas, L. G. Carbon Nanotube based Biomimetic Membranes: Mimicking Protein Channels Regulated by Phosphorylation. *J. Mater. Chem.* **2007**, *17*, 1755−1757.

(16) Majumder, M.; Zhan, X.; Andrews, R.; Hinds, B. J. Voltage Gated Carbon Nanotube Membranes. *Langmuir* **2007**, *23*, 8624−8631.

DOI: 10.1021/acsami.5b01183
ACS Appl. Mater. Interfaces 2015, 7, 14620−14627

(17) Wei, G. L.; Yu, H. T.; Quan, X.; Chen, S.; Zhao, H. M.; Fan, X. F. Constructing All Carbon Nanotube Hollow Fiber Membranes with Improved Performance in Separation and Antifouling for Water Treatment. *Environ. Sci. Technol.* **2014**, *48*, 8062−8068.
(18) Bastús, N. G.; Comenge, J.; Puntes, V. Kinetically Controlled Seeded Growth Synthesis of Citrate-Stabilized Gold Nanoparticles of up to 200 nm: Size Focusing versus Ostwald Ripening. *Langmuir* **2011**, *27*, 11098−11105.
(19) Voets, T.; Droogmans, G.; Wissenbach, U.; Janssens, A.; Flockerzi, V.; Nilius, B. The Principle of Temperature-Dependent Gating in Cold- and Heat-Sensitive TRP Channels. *Nature* **2004**, *430*, 748−754.
(20) Chang, G.; Spencer, R. H.; Lee, A. T.; Barclay, M. T.; Rees, D. C. Structure of the MscL Homolog from *Mycobacterium Tuberculosis*: A Gated Mechanosensitive Ion Channel. *Science* **1998**, *282*, 2220−2226.

DOI: 10.1021/acsami.5b01183
ACS Appl. Mater. Interfaces 2015, 7, 14620−14627